THE JOURNAL OF BIOLOGICAL CHEMISTRY VOL. 280, NO. 50, pp. 41429–41438, December 16, 2005

The Highly Abundant Protein Ag-lbp55 from *Ascaridia galli* Represents a Novel Type of Lipid-binding Proteins*

Received for publication, April 25, 2005, and in revised form, September 14, 2005 Published, JBC Papers in Press, October 6, 2005, DOI 10.1074/jbc.M504474200

Rositsa Jordanova[‡1], Georgi Radoslavov[‡], Peter Fischer[§2], Andrew Torda[¶], Friedrich Lottspeich[‖], Raina Boteva[**], Rolf D. Walter[§], Ilia Bankov[‡], and Eva Liebau[§3]

*From the [‡]Institute of Experimental Pathology and Parasitology, Sofia 1113, Bulgaria, [§]Bernhard Nocht Institute for Tropical Medicine, Hamburg 20359, Germany, [¶]Center for Bioinformatics, Hamburg University, Hamburg 20146, Germany, [‖]Max Planck Institute for Biochemistry, Martinsried 82152, Germany, and **National Center of Radiobiology and Radiation Protection, Sofia 1756, Bulgaria*

Lipid-binding proteins exhibit important functions in lipid transport, cellular signaling, gene transcription, and cytoprotection. Their functional analogues in nematodes are nematode polyprotein allergens/antigens and fatty acid and retinoid-binding proteins. This work describes a novel 55-kDa protein, Ag-lbp55, purified from the parasitic nematode *Ascaridia galli*. By direct N-terminal sequencing, a partial amino acid sequence was obtained that allowed the design of oligonucleotide primers to obtain the full-length cDNA sequence. Sequence analysis revealed the presence of an N-terminal signal peptide of 25 amino acid residues and a FAR domain at the C terminus. Data base searches showed almost no significant homologies to other described proteins. The secondary structure of Ag-lbp55 was predominantly α-helical (65%) as shown by CD spectroscopy. It was found to bind with high affinity fatty acids (caprylic, oleic, and palmitic acid) and their fluorescent analogue dansylaminoundecanic acid. Immunolocalization showed that Ag-lbp55 is a highly abundant protein, mainly distributed in the inner hypodermis and extracellularly in the pseudocoelomatic fluid. A similar staining pattern was observed in other pathogenic nematodes, indicating the existence of similar proteins in these species.

Parasitic nematodes are the most significant helminths in terms of numbers of species and distribution, causing many serious diseases in humans and animals. Furthermore, they have a great economic impact on many agricultural products. Differences between host and parasite biochemistry present possible targets for chemotherapy and are the object of intensive research in parasitology. In parasitic nematodes, specific metabolic pathways are modified to meet their actual physicochemical environment, the host organism. Because of the low oxygen tension in the host organs and tissues, helminths show a down-regulation of enzymes from the oxygen-dependent pathways, such as β-oxidation (1, 2). They exhibit restricted lipid metabolism but contain high levels of lipid as long chain fatty acids, retinoids, and steroids (1). The import of these metabolites from the host organism is essential for parasite survival, and consequently, the lipid transporters are possible targets for therapeutic agents (3).

The lipophilic ligands, such as long chain fatty acids, eicosanoids, retinoids, and steroids, play an important role in cellular homeostasis. Triacylglycerols are the major cell energy storage compounds. Some of the polyunsaturated fatty acids, retinoids, and steroids act as signaling molecules and take part in important cell processes such as gene transcription, cell development, inflammation, and immune response (4). As a consequence of their similar physical properties, principally hydrophobicity, these chemically and functionally different metabolites are unified into the group of "lipids." Because the tissue and cell environment is hydrophilic, these metabolites need to be solubilized and protected from chemical damage, and their transport and function have to be tightly regulated. The lipid-binding proteins (LBPs)[4] perform the important role of lipid carriers. Recently, proteins of the LBP family, related to the oxysterol-binding protein, were identified to play a major role in intracellular lipid targeting and are also structural components of the membrane contact sites (5, 6).

In vertebrates, three major structural groups of soluble LBPs are described, namely albumin, lipocalins, and cytosolic fatty acid-binding proteins (FABPs). Although lipocalins and FABPs are small β-sheet proteins (20 and 14 kDa, respectively), albumin is a larger α-helical protein (67 kDa) (7). Although mammalian FABPs are cytosolic and possess various tissue isoforms, lipocalins and albumin are involved in the extracellular lipid transport (8).

Nematodes secrete structurally different classes of small (15–20 kDa), helical lipid-binding proteins into host tissues, referred to as nematode polyprotein allergens/antigens (NPA) and fatty acid and retinoid-binding proteins (FAR) (9–11). The first representatives were identified as major nematode antigens (As-NPA-1 from *Ascaris suum* and Ov-FAR-1 from *Onchocerca volvulus*). They show a high affinity for amphipathic molecules, such as fatty acids and retinoids, and these features appear to be true for all members of both families (12–14). The completion of the genome from the model nematode *Caenorhabditis elegans* revealed eight FAR protein sequences, Ce-FAR-1 to 8 (11). Because FAR and NPA play a critical role in the fatty acid and retinoid import from the host and their ligands are essential for parasite survival, these proteins are of great interest. Additionally, a localized decrease of such lipids may have immunomodulatory effects that compromise the host immune response (1, 3).

* The costs of publication of this article were defrayed in part by the payment of page charges. This article must therefore be hereby marked "*advertisement*" in accordance with 18 U.S.C. Section 1734 solely to indicate this fact.

The nucleotide sequence(s) reported in this paper has been submitted to the GenBank™/EBI Data Bank with accession number(s) AY587609.

[1] Supported by Deutscher Akademischer Austausch Dienst and Deutsche Forschungsgemeinschaft. Recipient of the European Federation of Parasitologists Young Scientist Award, First Prize in Basic Parasitology, at the IX European Multicolloquium of Parasitology, Valencia, Spain, July 18–23, 2004. Present address: EMBL-Hamburg, Notkestrasse 85 (%DESY), Hamburg 22603, Germany.

[2] Present address: Infectious Diseases Division, Washington University School of Medicine, St. Louis, MO 63110.

[3] To whom correspondence should be addressed: Institute for Animal Physiology, University of Muenster, Hindenburgplatz 55, Muenster 48143, Germany. Tel.: 49-251-8321710; Fax: 49-251-83-21766; E-mail: liebaue@uni-muenster.de.

[4] The abbreviations used are: LBPs, lipid-binding proteins; NPA, nematode polyprotein allergens/antigens; FAR, fatty acid and retinoid-binding proteins; DAUDA, dansylaminoundecanic acid; MALDI-TOF, matrix-assisted laser desorption ionization time-of-flight; FABPs, fatty acid-binding proteins; RACE, rapid amplification of cDNA ends.

TABLE ONE

Oligonucleotide primers used to obtain the full length cDNA sequence of Ag-lbp55.
The specific primers for 3′- and 5′-RACE experiments are marked with asterisk (see text for details).

	Degenerate oligonucleotide primers
Forward	
S1	GA(A/G)GT(A/C/G/T)CA(C/T)GA(A/G)GA(C/T)(C/T)T(A/C/G/T)CA(C/T)CA(C/T)AT(A/C/T)GC
S2	CA(C/T)CA(C/T)AT(A/C/T)GC(A/C/G/T)AA(A/G)AA(A/G)AA(A/G)GC
S3	GA(C/T)CC(A/C/G/T)ATG(C/T)T(A/C/G/T)TA(C/T)GA(C/T)GG(A/C/G/T)GT(A/C/G/T)AC
S4	GC(A/C/G/T)AC(A/C/G/T)GA(C/T)TT(C/T)CA(C/T)GC(A/C/TG)(C/T)T(A/C/G/T)GC(A/C/G/T)CC(A/C/G/T)GA(C/T)GT
S5	GA(C/T)GC(A/C/G/T)GC(A/C/G/T)AT(A/C/T)GA(A/G)CT(A/G/C/T)GA(A/G)AA(A/G)GC
S6	GA(A/G)AA(A/G)GC(A/C/G/T)AA(A/G)CC(A/C/G/T)GG(A/C/G/T)GC(A/C/G/T)GA(C/T)AT(A/C/T)TA(C/T)G
Reverse	
AS1	GT(A/C/G/T)AC(A/C/G/T)CC(A/G)TC(A/G)TA(A/C/G/T)A(A/G)CAT(A/C/G/T)GG(A/G)TC
AS2	(C/T)TT(C/T)TG(A/C/G/T)A(A/G)(A/G)TT(C/T)TC(A/C/G/T)C(T/G)(A/G)AA
AS3	AC(A/G)TC(A/C/G/T)GG(A/C/G/T)GC(A/C/G/T)A(A/G)(A/C/G/T)GC(A/G)TG(A/G)AA(A/G)TC(A/C/G/T)GT(A/C/G/T)GC
AS4	GC(C/T)TT(C/T)TC(A/C/G/T)AC(C/T)TC(C/T)TC(T/G/A)AT(A/C/G/T)GC(A/C/G/T)GC(A/G)CT
AS5	C(A/G)TA(T/G/A)AT(A/G)TC(A/C/G/T)GC(A/C/G/T)CC(A/C/G/T)GG(C/T)TT(A/C/G/T)GC(C/T)TT(C/T)TC
	Specific oligonucleotide primers
Forward	
S11	CCAGTACATCTAAAACGTGAGTGTCAT
S22*	GAAACTGTTC AGAGAAGTTGTGGACTC
S33*	CATCATCAGGCGGACCAGGTTGCAGAG
S44	TGGGGAAGTCATCTTGATGT ATTC
Reverse	
AS11*	TAGAACATGAGCAAAACTTCT TGC
AS22*	ATGACACTCACGTTTTAGATGTACTGG
AS33	GAGTCCACAACTTCTCTGAACAGTTTC
AS44	GAATACATCAAGATGACTTCCCCA

In the chicken parasite, *Ascaridia galli*, the most abundant and prolific proteins have affinity for fatty acids. These are the NPA representative, Ag-NPA-1 (14, 15), and a novel 55-kDa protein, Ag-lbp55, that have no significant homology, besides a C-terminal FAR domain, with any proteins described so far. In the present study, Ag-lbp55 was purified, and its primary and secondary structures were identified. Its affinity for long chain fatty acids was studied by fluorescence spectroscopy. Furthermore, immunolocalization was performed, indicating an extracellular localization and the presence of similar proteins in other nematode parasites.

MATERIALS AND METHODS

Protein Purification—Native Ag-lbp55 was purified from adult *A. galli* worms, as described for Ag-NPA-1 (14, 16). The purification procedure included homogenization of the worms and ultracentrifugation and ammonium sulfate precipitation of the soluble protein fraction, followed by dialysis. The supernatant was further purified by anion exchange chromatography on DEAE-cellulose. The eluate was subjected to size exclusion chromatography on a Superdex 75 column. To avoid degradation of the native protein, all steps were performed at 4 °C and in the presence of the protease inhibitor (Complete Protease Inhibitor Mixture; Roche Applied Science). Additionally, a truncated form of the native protein was purified. The fatty acid binding activity during the purification procedure was checked by the binding of [^{14}C]palmitate (14, 16). The molecular size of the protein was determined by SDS-PAGE, using 12 and 4–20% gradient gels (Bio-Rad). The oligomeric state of the native protein in the presence or absence of ligand was studied by native gel electrophoresis, performed on 4–20% gradient gels as described in Ref. 17. The protein concentration was determined initially by the method of Bradford (18). After obtaining the amino acid sequence of Ag-lbp55, the concentration was also determined spectrophotometrically using a molar extinction coefficient of 32.79×10^3 M^{-1} cm^{-1} at 280 nm as calculated on the basis of the aromatic amino acid content of 3 Trp and 12 Tyr residues per protein monomer with ProtParam tool (www.expasy.org/).

The purity and homogeneity of the full-length protein were demonstrated by two-dimensional gel electrophoresis, performed according to the two-dimensional electrophoresis manual (Amersham Biosciences), and the protein bands were further analyzed by MALDI-TOF mass spectrometry. MALDI-TOF analysis of the peptides, obtained after tryptic digestion of Ag-lbp55 bands, was performed as described previously (17, 19). The data were additionally analyzed with PEPTIDE MASS software (www.expasy.org/).

CD Measurements—CD spectra were recorded in 10 mM Tris, pH 7.5, 20 °C, using a Jasco model 715 automatic recording CD spectrophotometer with a thermostatically controlled cell holder. A fused quartz cell with a path length of 0.1 cm was used. The protein concentration was 12.2 μM. The spectra, measured in the far UV-region of 190–260 nm, were averages of four scans and were corrected by subtracting the base line of the buffer. They are reported as mean residue molar ellipticity ($[\theta]_R$) in degrees cm^2 dmol^{-1}. Spectra subtraction, normalization, and smoothing were performed using Jasco CD J-715 data manipulation software, and the analyses of the data were carried out with the programs SELCON and CONTIN (20).

Peptide Sequencing—For internal sequencing, protein bands were cut out of the gel and digested with trypsin and the endoproteinases Lys-C and Asp-N (Roche Applied Science) as described (21). The obtained peptides were subjected to N-terminal sequencing and MALDI-TOF analysis. Microsequencing was performed using a gas-phase sequenator Procise 492 cLC (Applied Biosystems GmbH).

Nucleotide and Amino Acid Sequence—Based on the obtained N-terminal and internal peptide sequences, various combinations of degen-

erate oligonucleotides were designed, from the N-terminal sequence three forward primers S1, S2, and S3 and one reverse primer AS1, and from internal peptides three forward S4, S5, and S6 and four reverse primers AS2, AS3, AS4, and AS5 (TABLE ONE and Fig. 3). Total RNA was isolated from adult worms, using the TRIzol reagent (Invitrogen). Reverse transcription was performed with 4 μg of RNA, oligo(dT) primer, and Moloney-murine leukemia virus-reverse transcriptase (MBI) or Transcriptor Reverse Transcriptase (Roche Applied Science). Gene fragments were amplified from the cDNA preparation by PCR with random combinations of the forward and reverse degenerate primers, using PCR Supermix (Invitrogen). The annealing temperature was 55 °C. The PCR fragments were cloned into TOPO-TA-modified vector (pCR II, Invitrogen) and sequenced. The obtained sequence data were used to design new and specific oligonucleotide primers. Amplification with the standard PCR protocol of the *ag-lbp55* gene fragment and the internal regions of the degenerated primers was performed with the specific forward and reverse primers S11, S44, AS33, and AS44 (TABLE ONE and Fig. 3). The missing 5′ and 3′ ends of the cDNA from the *ag-lbp55* gene as well as the 5′- and 3′-degenerated oligonucleotide regions were isolated and sequenced using the 5′- and 3′-RACE methods, according to the manufacturer's manual (Invitrogen). The primers used for RACE experiments were S33 and S22 for the 3′-RACE and AS11 and AS22 for the 5′-RACE (TABLE ONE and Fig. 3). All oligonucleotides were purchased from Qiagen.

Deglycosylation—To investigate the existence of asparagine-linked glycan chains on Ag-lbp55, the *A. galli* extract was treated with *N*-glycosidase F (*N*-glycosidase F deglycosylation kit) according to the manufacturer's manual (Roche Applied Science). Following deglycosylation, treated and nontreated protein extracts were loaded on SDS-PAGE and transferred to a nitrocellulose membrane (Schleicher & Schuell). Ag-lbp55 was detected with mouse anti-Ag-lbp55 serum (see under "Immunohistology"), used at a 1:1000 dilution, and the second antibody was horseradish peroxidase-conjugated rabbit anti-mouse (Dako), used at a 1:10,000 dilution. Western blotting was prepared according to a standard protocol (22).

Data Analysis and Structure Predictions—Blast (23) and Psi-blast (24) were used for local sequence data base searches, and realignments were calculated using ClustalW (25). Searches of predefined sequence families were performed using the web interfaces to Pfam (26) the conserved domain data base (27) and SAM-T02 (28, 29). Molecular mass, molar extinction coefficient, and isoelectric point (pI) of the protein were estimated with the ProtParam program.

Ligand Binding Experiments and Reagents—The fluorescent fatty acid analogue 11-((5-dimethylaminonaphthalene-1-sulfonyl)amino)undecanoic acid (DAUDA) was obtained from Molecular Probes (Invitrogen). The fatty acids were products of Sigma. All ligands were dissolved in ethanol in concentrations of either 1 or 0.1 mM. The concentration of DAUDA was calculated from its absorption spectra, using the corresponding molar extinction coefficient of $4.8 \times 10^{-3}\ cm^{-1}\ M^{-1}$. Steady-state fluorescence was measured with a Shimadzu model RF5000 and PerkinElmer Life Sciences LS50B spectrofluorometers, equipped with a thermostatically controlled cuvette holder.

Ligand binding experiments were performed with 0.1 μm Ag-lbp55 and an initial sample volume of 800 μl. Binding affinities of Ag-lbp55 for fatty acids were studied by changes in the intrinsic tryptophan emission of the protein (excitation wavelength λ_{ex} of 295 nm and emission wavelength λ_{em} 340 nm). Binding of the fluorescent ligand DAUDA was monitored by measuring changes in its specific emission intensity (λ_{ex} 350 nm and $\lambda_{em(max)}$ 510 nm) that was expected to increase upon complex formation with the protein. Increasing amounts of fatty acids or

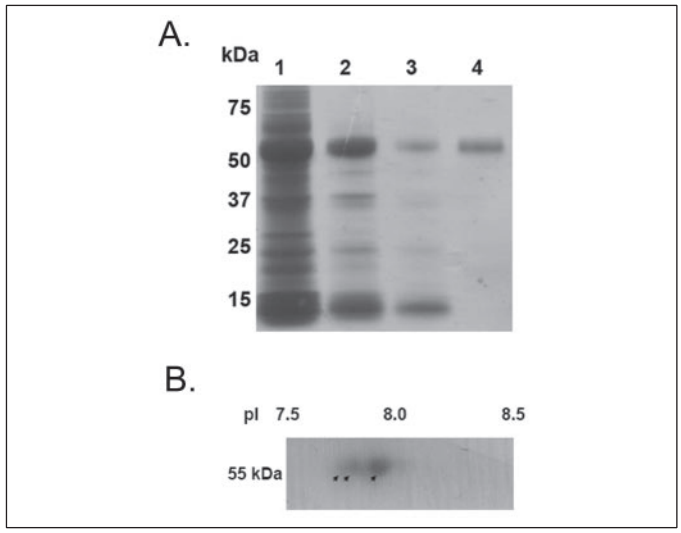

FIGURE 1. *A*, purification of Ag-lbp55 from *A. galli*, followed by SDS-PAGE. *Lane 1*, soluble protein fraction after ultracentrifugation (7.9 μg of protein); *lane 2*, supernatant after 70% saturation with ammonium sulfate (4.3 μg of protein); *lane 3*, eluted protein fraction after DEAE-cellulose chromatography (1.2 μg of protein); and *lane 4*, protein after Superdex 75 gel filtration (0.6 μg of protein). Proteins were visualized by Coomassie Blue staining. *B*, two-dimensional gel electrophoresis of Ag-lbp55. The three isoforms are marked with *arrows*.

DAUDA were added to Ag-lbp55, and the samples were equilibrated until a steady emission reading was obtained (usually 5 min). All titration experiments were performed in 10 mM Tris-HCl buffer, pH 7.5, at 20 °C. The concentration of the organic solvent in the final reaction did not exceed 2.5%. In order to minimize inner filter and self-absorption effects, absorbance of the samples at the excitation wavelength was always less than 0.05. Because DAUDA absorbs at the excitation wavelength (λ_{ex} 350 nm), its emission spectra were corrected for inner filter effects and background fluorescence. All emission spectra were corrected for progressive dilution (≈2.5% maximum) (30).

The apparent dissociation constants (K_d) and the maximal fluorescence change upon saturation of the Ag-lbp55-binding site (ΔF_{max}) were calculated from the experimental data with GraphPad Prism program. The data were analyzed by nonlinear regression and fitted to one-site binding hyperbola, by using Equation 1,

$$\Delta F_{obs} = \frac{F_{max}[L]}{K_d + [L]} \qquad \text{(Eq. 1)}$$

where ΔF_{obs} is the observed change in the fluorescence and [L] is the ligand concentration.

The stoichiometry of the complexes was computed by the Hill Equation 2 (31),

$$\frac{\log \Delta F}{1 - \Delta F} = \log K_d + n_H \log L \qquad \text{(Eq. 2)}$$

if ΔF_{max} represents saturation of all binding sites then ΔF corresponds to the fraction of full sites at certain ligand concentrations; $(1 - \Delta F)$ corresponds to the fraction of empty sites, and n_H is the Hill coefficient, which equals 1 if the stoichiometry of the protein-ligand complexes is 1:1.

Immunohistology—Antisera against Ag-lbp55 were raised in mice, using a standard immunization protocol (Eurogentec). The preimmune serum was used as a control. Immunolocalization on the light microscopic level was performed as described previously (15, 32). Anti-Ag-lbp55 serum was used as primary antibody at dilutions of 1:50 to 1:100.

TABLE TWO

N-terminal sequence of Ag-lbp55 and internal peptide sequences, determinated by Edman degradation

The fragments were obtained with proteolytic enzymes *Lys-C* and *Asp-N*, and *Asp-N*, respectively. For most of the peptides MALDI-TOF masses were obtained as well. The main part of the protein sequencing was done by Reinhard Mentele (MPI, Martinsried). (Also see Footnotes *a* and *b* below.)

Sequenced peptides	Mass from MALDI-TOF (Da)	Theoretical mass (Da)/comments
N-terminal sequence		
EVHEDLHHIAKKKARSFAHV		
Lys-C		
K16, FRENLQK	No mass	
K17, -	1327.7	Fits to N-terminal sequence
K18, AKPGADIYEETK	1321.6	1321.7
K21, LRDPMLYD*X*VTK	1446.9 + 1636.9	Fits not, glycosylated site
K23, ARSFAHVLSK	1115.6	1115.6
K24, same as K21		
K26, LATDFHALAPDVKK	1525.9	1525.9
GEHPSPEAFLK	1211.6	1211.6
K30, DENIHALQEVAAA	Total 3312.6	Average 3312.5
K33, TVTFPNALHLIQRYA..T	No mass	Glycosylated site
K41, HFPFRSILLFSTLD	1693	1692.9
Asp-N		
D10, DSAHGELA	799.25	799.35
D20, DENIHALQ	939.4	939.4
D31, DVFPQHFAH	1097.4	1097.5
D6, DEAKLKE	832.9	832.4
D7, EKLAT	No mass	
D22, DRKLFR	834.4	834.5
D44, DELINALFAGHSYLK	1690.9	1690.9
D33, ELSAKIRAIHV	1236.6	1236.7
D11, SLVEHE	No mass	
D25, DPMLY	No mass	
D28, DHVAMLRRYNELS	1619.7	1603.8 + 16 (Ox)
DAAIEEVEKAKPGA	1427.7	1427.7
D32, DRKLFRE	No mass	
D8, EEMTNLAK	No mass	
EKSPEK	No mass	
D24, EKAPRSHARAVILR	1603.9	1603.9
D35/36, DIMMLRSLVEHEH	1641.7	1609.8 + 32 (Ox)
D15, EVAAAHVHSP	1017.4	1017.5
D42, EEMTNLAKELSAKIRAIHV	2169.2	2153.2 + 16 (Ox)
D45, EVKAKNEKLYYILFLIN	2098.3	2098.2
Additional internal sequences		
LYYILFLINDHVAMLRRYNELSDPAEAFFH[a]		Contains D45 and D28
TVTFPNALHLIQRYA*X*TTEEYHHQADQVAEKLAT[a]		Contains K33, glycosylated site
DENIHALQEVAAAHVHSPD..HVN..[a]		Contains K30, D15, and D20
GKPAHPAH[b]		

[a] Additional internal sequences received from John Barrett (Institute of Biological Sciences, Aberystwyth).
[b] Additional peptide sequence received from Karlheinz Mann (Max Planck Institute, Martinsried).

As secondary antibody, goat anti-mouse antibody conjugated with alkaline phosphatase was employed, and Fast Red TR salt (Sigma) was used as the chromogen, whereas hematoxylin acted as the counterstain. For immunolocalization, adult *A. galli* worms were fixed in either 4% buffered formaldehyde or in 80% ethanol and embedded in paraffin. For comparison with other ascarids or with filarial nematodes, sections of female *A. suum* and of female *O. volvulus*, *Onchocerca gutturosa*, *Acanthocheilonema viteae*, and *Dirofilaria immitis* were used.

RESULTS

Protein Purification—Following gel filtration the native Ag-lbp55 was eluted as a single peak, corresponding to the molecular mass of the monomers, 55 kDa. By using the same procedure, another LBP from *A. galli*, the 15-kDa NPA representative, Ag-NPA-1, was purified (14, 15). These two proteins show the same biophysical and biochemical features, except that they differ in molecular masses, so their separation was possible by size exclusion chromatography. The binding activity of the eluted peaks was followed with [^{14}C]palmitate, and both proteins showed a high affinity for that ligand (data not shown). The native gel electrophoresis and gel filtration data indicate that under native conditions Ag-lbp55 is a monomer. The SDS-PAGE of the purification steps is shown in Fig. 1*A*. Moreover, Fig. 1*A*, *lane 1*, clearly shows that Ag-lbp55 together with the NPA protein are the most abundant and soluble *A. galli* proteins.

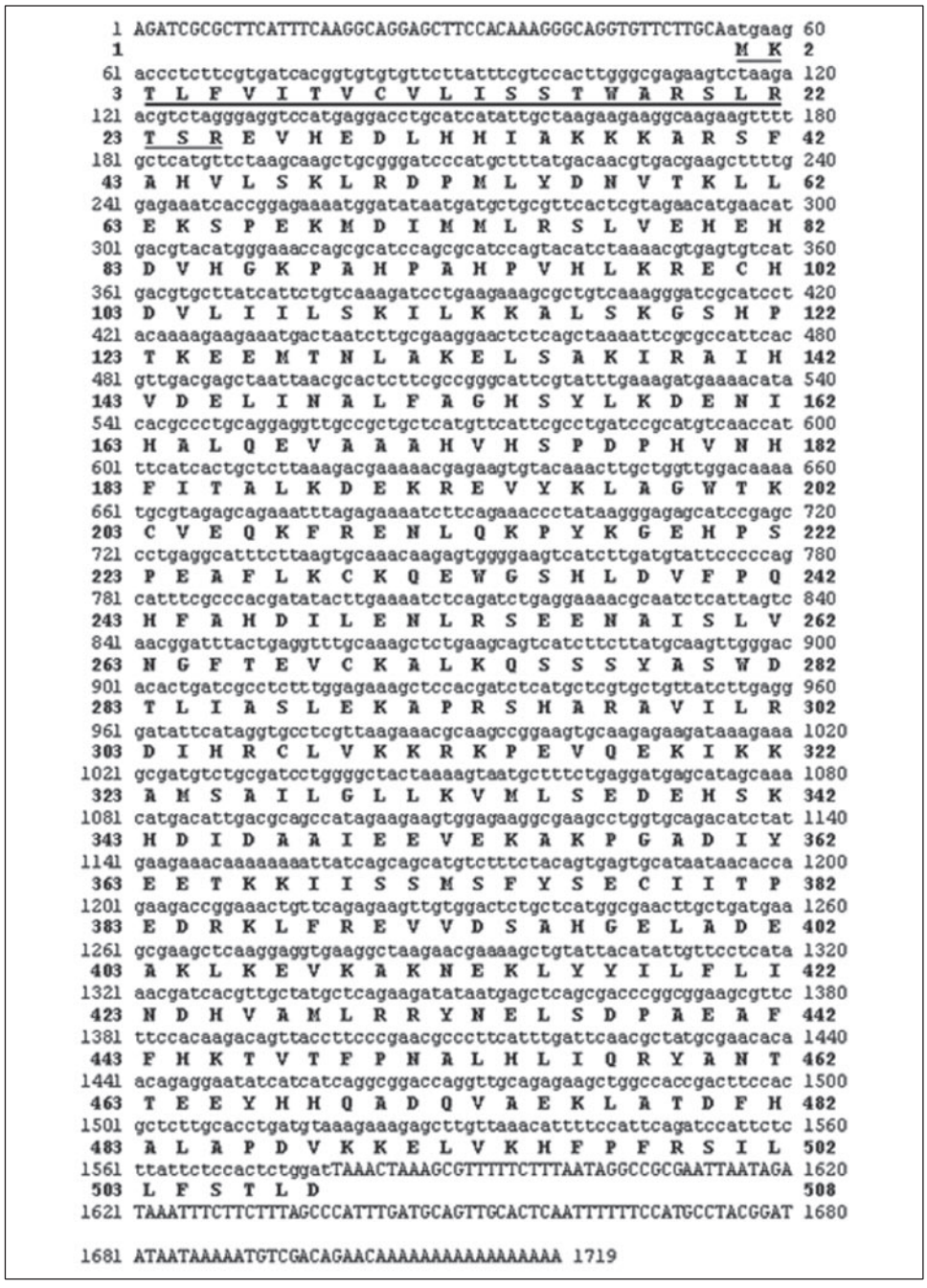

```
   1 AGATCGCGCTTCATTTCAAGGCAGGAGCTTCCACAAAGGGCAGGTGTTCTTGCAatgaag 60
   1                                                       M  K  2
  61 accctcttcgtgatcacggtgtgtgttcttatttcgtccacttgggcgagaagtctaaga 120
   3  T  L  F  V  I  T  V  C  V  L  I  S  S  T  W  A  R  S  L  R 22
 121 acgtctagggaggtccatgaggacctgcatcatattgctaagaagaaggcaagaagtttt 180
  23  T  S  R  E  V  H  E  D  L  H  H  I  A  K  K  K  A  R  S  F 42
 181 gctcatgttctaagcaagctgcgggatcccatgctttatgacaacgtgacgaagcttttg 240
  43  A  H  V  L  S  K  L  R  D  P  M  L  Y  D  N  V  T  K  L  L 62
 241 gagaaatcaccggagaaaatggatataatgatgctgcgttcactcgtagaacatgaacat 300
  63  E  K  S  P  E  K  M  D  I  M  M  L  R  S  L  V  E  H  E  H 82
 301 gacgtacatgggaaaccagcgcatccagcgcatccagtacatctaaaacgtgagtgtcat 360
  83  D  V  H  G  K  P  A  H  P  A  H  P  V  H  L  K  R  E  C  H 102
 361 gacgtgcttatcattctgtcaaagatcctgaagaaagcgctgtcaaagggatcgcatcct 420
 103  D  V  L  I  I  L  S  K  I  L  K  K  A  L  S  K  G  S  H  P 122
 421 acaaaagaagaaatgactaatcttgcgaaggaactctcagctaaaattcgcgccattcac 480
 123  T  K  E  E  M  T  N  L  A  K  E  L  S  A  K  I  R  A  I  H 142
 481 gttgacgagctaattaacgcactcttcgccgggcattcgtatttgaaagatgaaaacata 540
 143  V  D  E  L  I  N  A  L  F  A  G  H  S  Y  L  K  D  E  N  I 162
 541 cacgccctgcaggaggttgccgctgctcatgttcattcgcctgatccgcatgtcaaccat 600
 163  H  A  L  Q  E  V  A  A  A  H  V  H  S  P  D  P  H  V  N  H 182
 601 ttcatcactgctcttaaagacgaaaaacgagaagtgtacaaacttgctggttggacaaaa 660
 183  F  I  T  A  L  K  D  E  K  R  E  V  Y  K  L  A  G  W  T  K 202
 661 tgcgtagagcagaaatttagagaaaatcttcagaaaccctataagggagagcatccgagc 720
 203  C  V  E  Q  K  F  R  E  N  L  Q  K  P  Y  K  G  E  H  P  S 222
 721 cctgaggcatttcttaagtgcaaacaagagtggggaagtcatcttgatgtattcccccag 780
 223  P  E  A  F  L  K  C  K  Q  E  W  G  S  H  L  D  V  F  P  Q 242
 781 catttcgcccacgatatacttgaaaatctcagatctgaggaaaacgcaatctcattagtc 840
 243  H  F  A  H  D  I  L  E  N  L  R  S  E  E  N  A  I  S  L  V 262
 841 aacggatttactgaggtttgcaaagctctgaagcagtcatcttcttatgcaagttgggac 900
 263  N  G  F  T  E  V  C  K  A  L  K  Q  S  S  S  Y  A  S  W  D 282
 901 acactgatcgcctctttggagaaagctccacgatctcatgctcgtgctgttatcttgagg 960
 283  T  L  I  A  S  L  E  K  A  P  R  S  H  A  R  A  V  I  L  R 302
 961 gatattcataggtgcctcgttaagaaacgcaagccggaagtgcaagagaagatаaagaaa 1020
 303  D  I  H  R  C  L  V  K  K  R  K  P  E  V  Q  E  K  I  K  K 322
1021 gcgatgtctgcgatcctggggctactaaaagtaatgctttctgaggatgagcatagcaaa 1080
 323  A  M  S  A  I  L  G  L  L  K  V  M  L  S  E  D  E  H  S  K 342
1081 catgacattgacgcagccatagaagaagtggagaaggcgaagcctggtgcagacatctat 1140
 343  H  D  I  D  A  A  I  E  E  V  E  K  A  K  P  G  A  D  I  Y 362
1141 gaagaaacaaaaaaaattatcagcagcatgtctttctacagtgagtgcataataacacca 1200
 363  E  E  T  K  K  I  I  S  S  M  S  F  Y  S  E  C  I  I  T  P 382
1201 gaagaccggaaactgttcagagaagttgtggactctgctcatggcgaacttgctgatgaa 1260
 383  E  D  R  K  L  F  R  E  V  V  D  S  A  H  G  E  L  A  D  E 402
1261 gcgaagctcaaggaggtgaaggctaagaacgaaaagctgtattacatattgttcctcata 1320
 403  A  K  L  K  E  V  K  A  K  N  E  K  L  Y  Y  I  L  F  L  I 422
1321 aacgatcacgttgctatgctcagaagatataatgagctcagcgacccggcggaagcgttc 1380
 423  N  D  H  V  A  M  L  R  R  Y  N  E  L  S  D  P  A  E  A  F 442
1381 ttccacaagacagttaccttcccgaacgcccttcatttgattcaacgctatgcgaacaca 1440
 443  F  H  K  T  V  T  F  P  N  A  L  H  L  I  Q  R  Y  A  N  T 462
1441 acagaggaatatcatcatcaggcggaccaggttgcagagaagctggccaccgacttccac 1500
 463  T  E  E  Y  H  H  Q  A  D  Q  V  A  E  K  L  A  T  D  F  H 482
1501 gctcttgcacctgatgtaaagaaagagcttgttaaacattttccattcagatccattctc 1560
 483  A  L  A  P  D  V  K  K  E  L  V  K  H  F  P  F  R  S  I  L 502
1561 ttattctccactctggatTAAACTAAAGCGTTTTTCTTTAATAGGCCGCGAATTAATAGA 1620
 503  L  F  S  T  L  D                                          508
1621 TAAATTTCTTCTTTAGCCCATTTGATGCAGTTGCACTCAATTTTTTCCATGCCTACGGAT 1680

1681 ATAATAAAAATGTCGACAGAACAAAAAAAAAAAAAAAA 1719
```

FIGURE 2. **Nucleotide and derived amino acid sequence of Ag-lbp55.** The signal peptide is *underlined*. GenBank™ accession number is AY587609.

The two-dimensional gel electrophoresis analysis, in combination with MALDI-TOF analysis, demonstrated the homogeneity of the purified Ag-lbp55 fraction. The two-dimensional gel electrophoresis showed the presence of at least three isoforms with pI values of ~7.65, 7.7, and 7.8 (Fig. 1*B*). From the amino acid sequence of Ag-lbp55, the calculated pI is 6.99. The differences between calculated and measured pI values suggest post-translational modifications of the molecules, further supported by the presence of three isoforms. Subsequent proteolytic cleavage, followed by MALDI-TOF analysis of the obtained peptides confirmed that the three bands contain the same protein. These masses correspond to the one obtained from the digested Ag-lbp55 band, loaded on one dimensional SDS-PAGE. The mass spectrum of the tryptically cleaved Ag-lbp55 was compared with known parasitic or mammalian proteins, using the software MASCOT (33) (www.matrixscience.com), but no homology was observed.

Peptide Sequencing—In order to identify the purified protein and obtain some information on its amino acid sequence, N-terminal and internal peptide sequencing were performed. The sequence of the first amino acids of the native protein chain was obtained by direct N-terminal sequencing by Edman degradation and showed no homology with other described proteins. The N-terminal amino acid residue was glutamate and not the expected methionine, which suggested the presence of a signal peptide. In order to get more information about the amino acid sequence, the protein was proteolytically cleaved with trypsin and the endoproteinases Lys-C and Asp-N, and the obtained peptides were sequenced. This approach yielded 35 internal sequences, around 60% of the total protein sequence (TABLE TWO). The mass and the accuracy of most of the sequences were confirmed by mass spectroscopic MALDI-TOF analysis (TABLE TWO). Some of the peptides obtained with different proteases overlapped, allowing identification of the first

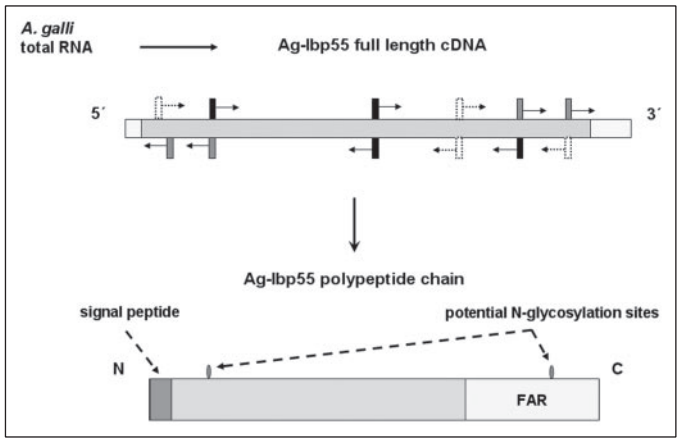

FIGURE 3. **Cloning strategy and organization of *ag-lbp55* gene and protein chain.** Full-length cDNA sequence was obtained using degenerated (*white* and *arrow*) and specific (*black* and *arrow*) oligonucleotides. The specific primers for 3′- and 5′-RACE are marked in *gray* and *arrow*, the noncoding 3′ and 5′ regions are shown in *white*. The signal peptide of the translated protein sequence, the recognized FAR domain, and the two potential *N*-glycosylation sites are shown.

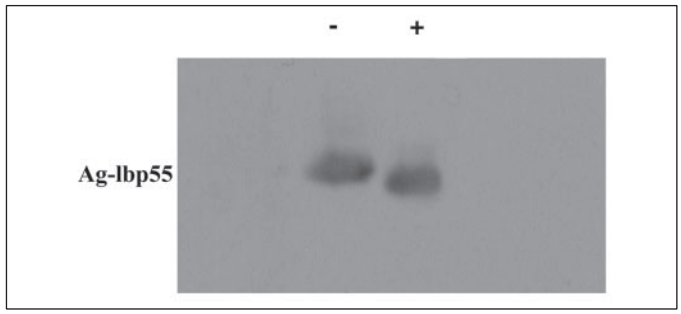

FIGURE 4. **Western blot showing deglycosylation of Ag-lbp55 with *N*-glycosidase F.** *1st lane* (−), undigested protein; *2nd lane* (+), digested protein.

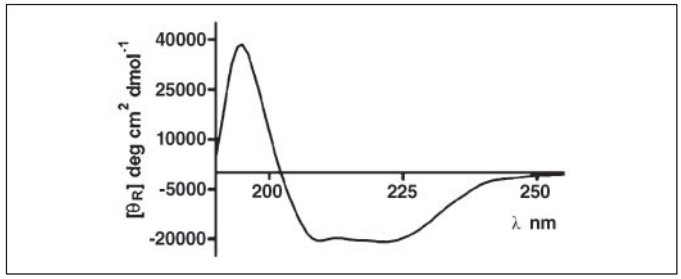

FIGURE 5. **CD spectrum of Ag-lbp55 in the far-UV region (190–260 nm).**

35 N-terminal residues. Most interestingly, the amino acid residues at position 32 and 436 could not be identified, due to a post-translational modification. After obtaining the cDNA sequence, these were found to be asparagine residues, and the sites were identified as potential *N*-glycosylation sites (Figs. 2 and 3).

Glycosylation of Ag-lbp55—The post-translational modification of Ag-lbp55 in the form of *N*-glycosylation was investigated by digesting the protein with the endoglycosidase *N*-glycosidase F. Fig. 4 shows a Western blot in which the native Ag-lbp55 was detected with anti-Ag-lbp55 serum before (Fig. 4, *1st lane*) and after (*2nd lane*) cleavage by the enzyme *N*-glycosidase F. The presence of oligosaccharides in protein molecule is clearly indicated by the observed size difference.

Primary Structure—Initially, two neighboring PCR fragments of the *ag-lbp55* gene, ~1000 and 500 bp, were amplified. The 1000-bp fragment was amplified with the N terminus-based S1 forward primer and AS4 and AS5 reverse primers, and 500-bp fragment was obtained with S5 and S6 forward and AS3 reverse primers. Based on these sequences, specific primers were designed, and the main gene fragment was amplified by standard PCR. The following 5′- and 3′-RACE results revealed the full-length cDNA sequence. The *ag-lbp55* gene identification strategy is shown in Fig. 3. The nucleotide sequence consists of 1719 bp and contains both the 5′- and the 3′-noncoding regions (Figs. 2 and 3). The transcript has a single open reading frame, which translates into 508 amino acids that compose the full-length protein (Fig. 2). The sequence of Ag-lbp55 has been deposited in GenBank™ under accession number AY587609. The full-length protein starts with a 25-amino acid signal peptide that indicates an extracellular localization. As mentioned above, the protein sequence contains two *N*-glycosylation sites at positions 32 and 436, respectively (Fig. 2). The molecular mass of the native protein was calculated at 55,396 Da, a value similar to the experimentally obtained data.

A simple sequence data base search using Blast or Psi-blast with Ag-lbp55 against the nonredundant sequence data base reveals no homologues at all, which one would normally consider reliable. There are no homologues with an expectation value (*e*-value) less than 0.08 and, consequently, no hits that would be included in a Psi-blast profile using even a loose acceptance criterion. The weak hits found with *e*-values $\approx 10^{-1}$ are in the N-terminal half of the sequence and include a likely nuclear hormone receptor (E75_CHOFU) and genes annotated as RNA helicases. These are statistically not significant. The list also includes several fatty acid and retinoid (FAR)-binding proteins possibly related to the C-terminal half of Ag-lbp55 with even weaker *e*-values. The closest homologue, Wb-FAR-1 from *Wuchereria bancrofti* (accession Q8WT54), had only 27% sequence identity to the C-terminal Ag-lbp55 region from residues 359 to 497. This, however, was significant as explained below.

Searching against one set of precomputed domain profiles (27) or hidden Markov models (28, 29) with Ag-lbp55 provides no hits of significance, but a search of Pfam (26) finds the family labeled gp-FAR-1 with an *e*-value of 6×10^{-3}. This led to a very directed and controlled search. A sequence profile was constructed in Psi-blast, based on the 178 residues of Wb-FAR-1 protein precursor using an acceptance criterion of 5×10^{-13} and just two rounds of homologue collection. This is exactly 10 orders of magnitude more conservative than the Psi-blast default. This sequence profile returns a hit to Ag-lbp55 with an *e*-value of 2×10^{-5}. Obviously with this stringent criterion for profile construction and the very low expectation value, there is little room for doubt. Ag-lbp55 contains a sub-sequence very distantly related to the set of FAR proteins, including Wb-FAR-1. The profile contained 30 proteins either annotated as FAR proteins or not yet annotated.

Secondary Structure—The sequence of Ag-lbp55 was given to several secondary structure prediction programs, using their web interfaces (34–37). This produced a very clear result. Almost every region with any predicted secondary structure was most likely to be α-helical. To be strictly correct, Profsec predicted only 15 β-strand residues, mostly in the presumed signal peptide. Psipred predicted six β-strand residues. It did not even predict residues anywhere else that could join to form a β-sheet. It is fair to conclude that on the basis of predictions, this protein and any constituent domains are most likely all α-helical. CD spectroscopy in the far-UV region (190–260 nm) generally agrees (Fig. 5), predicting ~65% α-helical structure. β-Structures and coil were estimated at ~17 and 18%, respectively.

Binding of Fatty Acids and DAUDA—The fluorescence properties of Ag-lbp55 are determined by its three Trp and 12 Tyr residues. Its fluorescence emission spectra were dominated by Trp emission. Binding of

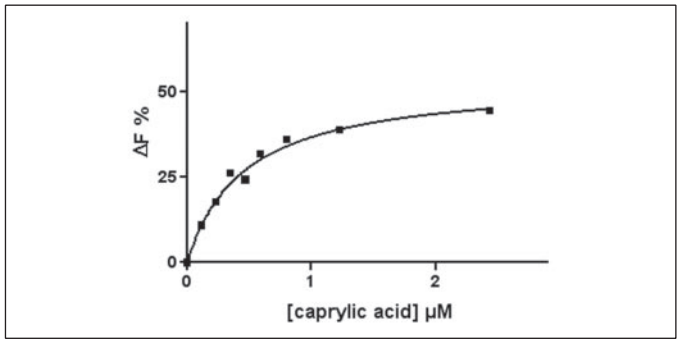

FIGURE 6. **Binding of caprylic acid to Ag-lbp55, followed by the changes of the Trp emission of the protein at 340 nm after excitation at 295 nm.** The derived curve is fitted by a nonlinear regression for a single binding site, and the calculated K_d value is 0.36 ± 0.10 μM.

fatty acids, varying in length and saturation, caused significant changes in Trp fluorescence expressed in enhancement and approximately a 10 nm red-shift of the Trp emission of Ag-lbp55 from 330 to 340 nm. The dissociation constant (K_d), the maximum fluorescence change upon saturation of the binding sites (ΔF_{max}), and the Hill coefficient (n_H) were calculated from the fluorescence enhancement at 340 nm. Analysis of the fluorescence-binding isotherms showed that the protein has one binding site shared by caprylic ($n_H = 1.1 \pm 0.4$), oleic ($n_H = 1.0 \pm 0.1$), and palmitic acids ($n_H = 1.0 \pm 0.1$). For the first two acids (caprylic and oleic), we estimated quite similar values for K_d of 0.36 ± 0.10 and 0.19 ± 0.05 μM, whereas palmitic acid was bound with almost an order of magnitude lower affinity, K_d of 1.26 ± 0.18 μM. Binding of the tested fatty acids caused similar enhancement of Trp fluorescence (ΔF_{max}), reaching up to 50–60%. The saturation of the Ag-lbp55 affinity site with fatty acids followed a hyperbolic curve as shown by the example binding curve for caprylic acid in Fig. 6.

Binding of DAUDA to Ag-lbp55 caused a relatively small increase of the fluorescence intensity of the dye (up to 28%) and 9 nm blue-shift of the emission maximum position, suggesting a rather polar environment of the probe, which is most probably located close to the surface of the protein molecule. The hyperbolic shape of the titration curve again suggested the existence of one class of high affinity binding site with a K_d of 0.14 ± 0.03 μM.

Immunohistology—By using the Ag-lbp55 antiserum, worms fixed either with ethanol or formalin were stained. The preimmune serum, which was employed as a negative control, showed a complete absence of unspecific reactions (Fig. 7*A*). By using the Ag-lbp55 antiserum, intense staining of the fluid in the pseudocoelomatic cavity of *A. galli* was observed (Fig. 7*B*). A weaker staining was observed in the lumen of the intestine, although no staining of the intestinal wall, the muscle syncytia, the uterus, and the ovary was detected. Intracellularly, staining for Ag-lbp55 was found especially in the inner hypodermis (Fig. 7, *C* and *D*). A similar staining pattern was found in the closely related species *A. suum*, with strong labeling of the median (Fig. 7*F*) and lateral cords. These results confirm the finding that Ag-lbp55 is one of the most abundant proteins in *A. galli* and also show an extracellular distribution, similar to that of the other LBP-Ag-NPA-1 (15) (Fig. 7, *A–D*).

The staining pattern of the anti-Ag-lbp55 serum in the ascarid worms was compared with the one in filarial nematodes, which included the agent of human riverblindness *O. volvulus*, the related cattle parasite *O. gutturosa*, the rodent parasite *A. viteae,* and the dog heartworm *D. immitis*. A similar staining pattern was observed in all species, indicating the presence of similar proteins that cross-react with Ag-lbp55 antiserum (Fig. 8). Extracellular staining of the pseudocoelom was observed in some sections (Fig. 8*A*), but not in all (Fig. 8*B*), because pseudocoelomatic fluid appeared to be not preserved in these sections. Additional labeling of the inner uterus epithelium was observed in female *O. gutturosa* with empty uterus branches (Fig. 8*B*), although in a few cases, in *D. immitis*, a weak to moderate staining of the inner epithelium and the lumen of the intestine was seen (Fig. 8*D*).

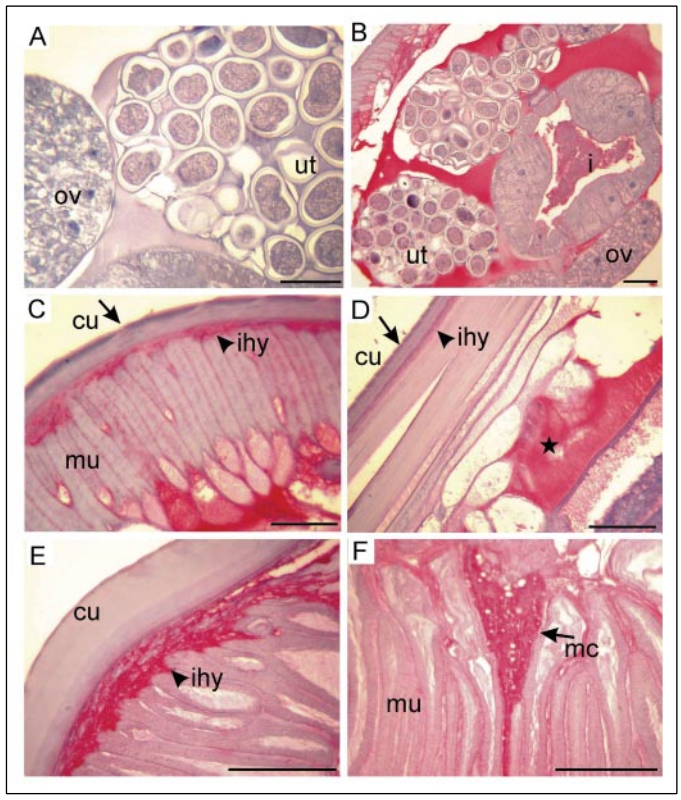

FIGURE 7. **Immunohistological localization of Ag-lbp55 in *A. galli* (*A–D*) and comparison with that in *A. suum* (*E–F*).** The localization of Ag-lbp55 in adult worms was performed with a polyclonal mouse antiserum raised against the native protein (dilutions 1:100 in *A–D* and 1:50 in *E–F*). *A*, preimmune serum showing no labeling of the pseudocoelomatic fluid, the ovary (*ov*), and the uterus (*ut*). *B*, consecutive section to *A* but stained with anti-Ag-lbp55 showing intensive *red* staining of the pseudocoel, weak staining of the lumen of the intestine (*i*), and no labeling of the uterus and ovary. *C*, strong labeling of the inner hypodermis (*arrowhead, ihy*) and space between the striate musculature (*mu*). No labeling was observed within the cuticle (*cu*), and only a weak staining was observed in the epicuticle (*arrow*). *D*, longitudinal section showing *red* labeling of the inner hypodermis and the pseudocoel (*star*). *E*, cross-section of *A. suum* indicating strong labeling of the inner hypodermis (*arrowhead*). *F*, same section as *E* showing strong labeling of the median cord (*arrow, mc*). *Bar size* is 50 μm.

DISCUSSION

Ag-lbp55 is the first described 55-kDa nematode protein that exhibits an affinity for amphipathic molecules. It was initially isolated during the purification of Ag-NPA-1 (14, 15), and an affinity for both radioactive palmitate and dansylated fatty acid DAUDA was demonstrated. Direct N-terminal sequencing showed that it differed from the polyprotein units, but the sequence could not be identified (14). The protein contains ~65% α-helices (Fig. 5), a secondary structure organization similar to that of FAR and NPA representatives (3, 9, 11) and is probably a new structurally unique class within LBPs.

Two-dimensional gel electrophoresis shows the presence of different isoforms of Ag-lbp55 with pI of ~7.65, 7.7, and 7.8, respectively. Tryptic digestion and MALDI-TOF analysis of the different bands revealed that they all contain only Ag-lbp55. The experimentally observed pI values differ from the theoretically predicted value of 6.99, which is probably a result of protein folding or post-translational modifications. The presence of isoforms might be due also to saturation of some binding sites

with ligand(s), and as a result the purified protein fraction would contain differently charged molecule species.

The FAR and NPA proteins are major allergens in helminths and are found in their excretory/secretory products. Sequencing suggested modifications of Asn-32 and Asn-436, and further analysis showed that Ag-lbp55 is glycosylated. Such a glycosylation is typical for secretory proteins, and some of the filarial FAR proteins are found to be glycosylated (38). The tissue localization of the protein in *A. galli* showed similar distribution to the NPA polyprotein (15). The antiserum did not cross-react with the NPA or any other protein from the worm extract, and only areas rich in Ag-lbp55 were stained. Although there are some findings that NPA and FAR proteins interact directly with membranes (39), an undiscovered membrane receptor possibly exists. Ag-lbp55 would be suited for this function, but the pseudocoelomic distribution shows that it is mainly extracellularly localized, and only in a few sections was a staining of the inner uterus epithelium or of the inner epithelium of the intestine observed. Even though Ag-lbp55 might be a soluble receptor, no direct interaction between it and Ag-NPA-1 was found. The Ag-lbp55 antiserum cross-reacted with sections from *A. suum*, *O. volvulus*, *O. gutturosa, A. viteae,* and *D. immitis,* and a similar staining pattern was observed. Localization of Ag-lbp55 and Ag-NPA-1 (15) in the hypodermis is similar to the FAR distribution found in filarial nematodes (40). Nevertheless, a Western blot with filarial extracts showed protein bands at higher molecular mass than the FAR size of 20 kDa (data not shown). Therefore, we propose that the antiserum recognizes analogues of Ag-lbp55 in the filarial parasites.

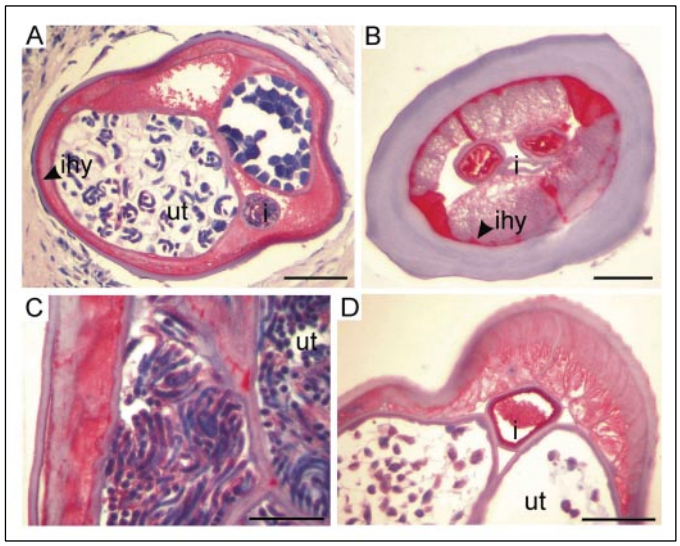

FIGURE 8. **Identification of cross-reactive proteins in filarial nematodes using the antiserum against Ag-lbp55.** *A*, cross-section of a female *O. volvulus* showing labeling of the inner hypodermis (*arrowhead, ihy*) and pseudocoelomatic fluid. No labeling was observed in the uterus (*ut*) and the wall of the intestine (*i*). *B*, cross-section of the cattle parasite *O. gutturosa* demonstrating strong labeling of the inner hypodermis (*arrowhead, ihy*) and the median and lateral cords. The inner epithelium of the uterus was also stained, but not the intestine (*i*). *C*, also in the rodent filaria *A. viteae* the inner hypodermis and the pseudocoel was labeled. *D*, a similar staining pattern was also observed in the dog heartworm *D. immitis* with additional staining of the inner epithelium of the intestine (*i*) and the lumen of the intestine. Antiserum was used at a dilution of 1: 50, *bar size* is 50 μm.

Aside from the physical-chemical properties of the protein, one may ask what can be stated based on its sequence. This could be summarized by saying that Ag-lbp55 appears to be a new type of fatty acid and retinoid-binding protein, with two or more largely α-helical domains and a unique N-terminal region about which one can only speculate. These conclusions can be easily justified. One can begin with the proposition that this is a new kind of FAR protein and remember that the homology to other FAR proteins is so remote that its *e*-value would normally be dismissed. It is only via a reverse, profile-based search, seeded from an annotated FAR domain, that one can see the relationship to Ag-lbp55. The weakness of the relationship also means that it would be dangerous to over-interpret the results. A Psi-blast profile suggests Ag-lbp55 has 27% sequence identity to Wb-FAR-1 and that the segment runs from residues 359 to 497. With ClustalW (25), one can more carefully recalculate alignments and align a few more residues (from position 358). The alignments, however, are not stable in the face of different penalties or substitution matrices (results not shown), so it

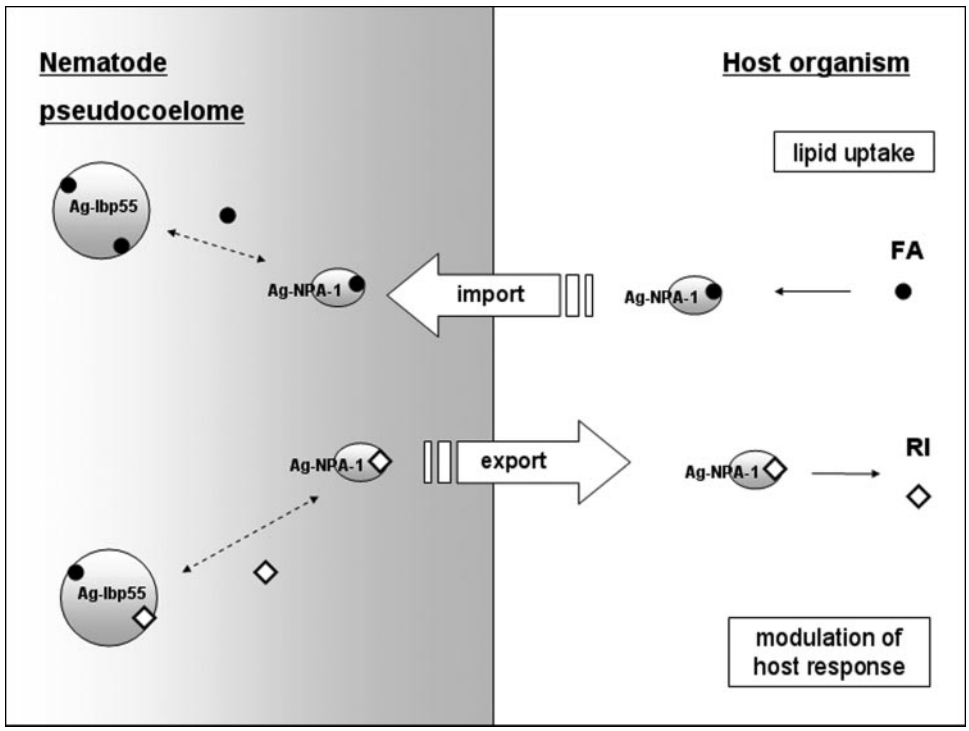

FIGURE 9. **Possible mode of action of *A. galli* LBPs in the lipid host-parasite-host trafficking (see text for details).** *RI,* retinoid; FA, fatty acid.

would be premature to discuss Ag-lbp55 in terms of conserved residues. This will change as the data bases contain more sequences and one can build a profile that better covers sequence space near Ag-lbp55.

For the C-terminal region, one may ask what can be said in structural terms. There are no known structures of any related sequences. The secondary structure predictions suggest this region is entirely α-helical, and the CD spectroscopy suggests it is largely helical. The sequence of Ag-lbp55 was also given to a barrage of protein fold recognition servers (FFAS (41), wurst (42), 3DPSSM (43), GenTHREADER (44), and Fugue (45)), but this yielded absolutely no consensus beyond the fact that all high-ranked guesses from all servers were entirely α-helical proteins. A cynic may note that many of these servers do use an initial secondary structure prediction as part of their calculations, so the result may not be a surprise.

This leads to the question of the N-terminal 358 residues and what similarity can be found. On the basis of the simple sequence searches, there are no homologues of statistical significance. Searching against precomputed families (26, 27) finds no similarities. Finally, sequence profiles were built, seeded by the sequences corresponding to the very weak hits mentioned above (RNA helicase and nuclear hormone receptor). These profiles do not return any plausible similarities to Ag-lbp55. The protein fold recognition servers do not even provide any consensus as to SCOP (46) or CATH (47) grouping. It was stated above that Ag-lbp55 is unusual because its only homology is weak and limited to the C-terminal region. One can now go further and say it seems to be the first example of a FAR protein with an extra N-terminal domain(s) of unknown structure and function.

One can finish the discussion of the sequence with some pure speculation. A simple blast search using Ag-lbp55 aligns residues 20–157 to a sequence known as E75_CHOFU (accession gb AAB52717.1), but with an *e*-value one would normally dismiss as insignificant (0.1). E75_CHOFU, however, is part of a large family of proteins involved in steroid and lipid binding, transport, and import. The group of related sequences even includes many structures (all α-helical proteins). It is certainly attractive to propose some fatty acid transport role for this stretch of sequence, but at the moment, there is no good statistical evidence.

The LBP proteins are highly expressed in adult *A. galli* possibly pointing to the essential function within the mature worm. The parasitic stages of nematodes cannot synthesize long chain fatty acids and steroids *de novo*, lack functional β-oxidation, and consequently, cannot catabolize these metabolites (1). However, parasitic helminths accumulate fatty acids, steroids, and fat-soluble vitamins and therefore exhibit a nutritional requirement for exogenous lipids. In nematodes, lipids are found in muscles, lateral chord, reproductive organs, and the intestine. In infective larvae, the intestine has been proposed as an important lipid storage place (1). In adult *A. galli,* the LBP distribution correlates well with the places of lipid accumulation, which is an indication for their importance in internal lipid trafficking and targeting in adult parasites. Additionally, it could be assumed that these or other LBPs are active in distinct larval stages of the nematode because metabolism of many helminths changes from aerobic to anaerobic during their development (1). Differences in the type and level of expressed LBPs in the larval and adult stage of the parasite *Trichinella spiralis* were found by data base mining.[5] Because of the limited ability of helminths to synthesize long chain fatty acids and steroids and the necessity to import them from the host organism, there is a need for finely regulated storage and traffic of these metabolites.

As mentioned above, both LBPs are the most abundant soluble proteins in *A. galli*. They share identical biochemical and biophysical properties, belong to the structural family of "all α" proteins, and have similar distribution and affinity for fatty acids. The high levels of Ag-lbp55 in *A. galli* extract and the abundant distribution suggest an essential function(s) in nematode lipid metabolism, perhaps regulating the lipid host-parasite-host trafficking as well. This raises the question as to why the nematode needs two proteins with affinity for hydrophobic ligands and what is the relation between them. If Ag-NPA-1 simply binds and transports lipids, Ag-lbp55 could act as a reservoir of these molecules in the pseudocoelome fluid. It would regulate the lipid levels in the parasite tissue by binding and/or releasing the necessary metabolites for the functional stage (Fig. 9). Although a direct interaction between both LBPs was not observed, it is possible that an intermediate protein exists. In contrast to Ag-NPA-1, Ag-lbp55 is too big to pass through membranes, and according to the localization data, it is not membrane-bound. However, it might act as a soluble receptor or interact with a still unidentified membrane receptor. It was shown that the family of LBP related to oxysterol-binding proteins is involved in the cellular nonvesicular traffic of lipids. They fulfill the two functions of lipid binding and applying selectivity to the lipid traffic, and moreover, they are structural components of the membrane contact sites (5, 6).

One of the highest requirements of a parasite worm is to take up lipid and other essential metabolites from the host organism and to prevent or escape the host response. Expression of several proteins with specific transport function could be part of an evolutionary adaptation to the parasitic mode of life. Another adaptation would be to combine several activities of a reduced metabolic pathway to just one protein, separated on different domains. Finally, the sheer abundance of Ag-lbp55 and its affinity for fatty acids suggest its importance for lipid homeostasis in the nematode, but there is much room for further work. One would like to confirm or rule out interactions with other proteins, and it could be that either conventional biochemistry or simply the cataloguing of more sequences will help find a role for the N-terminal 3/5 of the protein.

Acknowledgments—We thank Elisabeth Weyher-Stingl (Max Planck Institute, Martinsried, Germany) for help with CD measurements and data interpretation. We thank John Barrett (Institute of Biological Sciences, University of Wales, Aberystwyth, United Kingdom), Karlheinz Mann (Max Planck Institute, Martinsried), and Reinhard Mentele (Max Planck Institute, Martinsried) for the protein sequencing. We also thank Joachim Clos (Bernhard Nocht Institute, Hamburg, Germany) for preparing the MALDI-TOF experiments, Insa Bonow (Bernhard Nocht Institute, Hamburg) for the assistance with immunohistology, and Christina Mertens and Manfred Uphoff (Intervet GmbH) for the A. galli samples.

[5] G. Radoslavov, unpublished data.

REFERENCES

1. Barrett, J. (2001) in *Perspectives on Helminthology* (Chowdhury, N., and Tada, I., eds) pp. 309–334, Science Publishers Inc., Enfield, NH
2. Tielens, A. G. (1994) *Parasitol. Today* **10,** 346–352
3. Kennedy, M. W. (2001) in *Parasitic Nematodes: Molecular Biology, Biochemistry and Immunology* (Kennedy, M. W., and Harnett, W., eds) pp. 309–330, CABI Publishing, Wallingford, UK
4. Noy, N. (2000) *Biochem. J.* **348,** 481–495
5. Loewen, C. J., Roy, A., and Levine, T. P. (2003) *EMBO J.* **22,** 2025–2035
6. Levine, T. (2004) *Trends Cell Biol.* **14,** 483–490
7. Wilton, D. C. (1990) *Biochem. J.* **270,** 163–166
8. Zimmerman, A. W., and Veerkamp, J. H. (2002) *Cell. Mol. Life Sci.* **59,** 1096–1116
9. Kennedy, M. W. (2000) *Biochim. Biophys. Acta* **1476,** 149–164
10. McDermott, L., Cooper, A., and Kennedy, M. W. (1999) *Mol. Cell. Biochem.* **192,** 69–75
11. Garofalo, A., Rowlinson, M. C., Amambua, N. A., Hughes, J. M., Kelly, S. M., Price, N. C., Cooper, A., Watson, D. G., Kennedy, M. W., and Bradley, J. E. (2003) *J. Biol. Chem.* **278,** 8065–8074

12. Kennedy, M. W., Brass, A., McCruden, A. B., Price, N. C., Kelly, S. M., and Cooper, A. (1995) *Biochemistry* **34,** 6700–6710
13. Kennedy, M. W., Garside, L. H., Goodrick, L. E., McDermott, L., Brass, A., Price, N. C., Kelly, S. M., Cooper, A., and Bradley, J. E. (1997) *J. Biol. Chem.* **272,** 29442–29448
14. Timanova, A., Muller, S., Marti, T., Bankov, I., and Walter, R. D. (1999) *Eur. J. Biochem.* **261,** 569–576
15. Jordanova, R., Radoslavov, G., Fischer, P., Liebau, E., Walter, R. D., Bankov, I., and Boteva, R. (2005) *FEBS J.* **272,** 180–189
16. Timanova, A. M., Marti, T., Walter, R. D., and Bankov, I. Y. (1997) *Parasitol. Res.* **83,** 518–521
17. Clos, J., Westwood, J. T., Becker, P. B., Wilson, S., Lambert, K., and Wu, C. (1990) *Cell* **63,** 1085–1097
18. Bradford, M. M. (1976) *Anal. Biochem.* **72,** 248–254
19. Stone, K. L., and Williams, K. R. (1986) *J. Chromatogr.* **359,** 203–212
20. Provencher, S. W. (1982) *Comput. Phys. Commun.* **27,** 229–242
21. Eckerskorn, C., and Lottspeich, F. (1993) *Electrophoresis* **14,** 831–838
22. Sambrook, J., Fritsch, E. F., and Maniatis, T. (1989) *Molecular Cloning: A Laboratory Manual*, 2nd Ed., pp. 18.60–18.75, Cold Spring Harbor Laboratory Press, NY
23. Altschul, S. F., Gish, W., Miller, W., Myers, E. W., and Lipman, D. J. (1990) *J. Mol. Biol.* **215,** 403–410
24. Altschul, S. F., Madden, T. L., Schaffer, A. A., Zhang, J., Zhang, Z., Miller, W., and Lipman, D. J. (1997) *Nucleic Acids Res.* **25,** 3389–3402
25. Thompson, J. D., Higgins, D. G., and Gibson, T. J. (1994) *Nucleic Acids Res.* **22,** 4673–4680
26. Bateman, A., Coin, L., Durbin, R., Finn, R. D., Hollich, V., Griffiths-Jones, S., Khanna, A., Marshall, M., Moxon, S., Sonnhammer, E. L. L., Studholme, D. J., Yeats, C., and Eddy, S. R. (2004) *Nucleic Acids Res.* **32,** D138–D141
27. Marchler-Bauer, A., Anderson, J. B., Cherukuri, P. F., DeWeese-Scott, C., Geer, L. Y., Gwadz, M., He, S., Hurwitz, D. I., Jackson, J. D., Ke, Z., Lanczycki, C. J., Liebert, C. A., Liu, C., Lu, F., Marchler, G. H., Mullokandov, M., Shoemaker, B. A., Simonyan, V., Song, J. S., Thiessen, P. A., Yamashita, R. A., Yin, J. J., Zhang, D., and Bryant, S. H. (2005) *Nucleic Acids Res.* **33,** D192–D196
28. Park, J., Karplus, K., Barrett, C., Hughey, R., Haussler, D., Hubbard, T., and Chothia, C. (1998) *J. Mol. Biol.* **284,** 1201–1210
29. Karplus, K., Barrett, C., and Hughey, R. (1998) *Bioinformatics* **14,** 846–856
30. Lehrer, S. S. (1971) *Biochemistry* **10,** 3254–3263
31. Monod, J., Wyman, J., and Changeux, J. P. (1965) *J. Mol. Biol.* **12,** 88–118
32. Fischer, P., Schmetz, C., Bandi, C., Bonow, I., Mand, S., Fischer, K., and Buttner, D. W. (2002) *Exp. Parasitol.* **102,** 201–211
33. Perkins, D. N., Pappin, D. J., Creasy, D. M., and Cottrell, J. S. (1999) *Electrophoresis* **20,** 3551–3567
34. Rost, B. (1996) *Comput. Methods Macromol. Sequence Anal.* **266,** 525–539
35. Cuff, J. A., and Barton, G. J. (2000) *Proteins* **40,** 502–511
36. McGuffin, L. J., Bryson, K., and Jones, D. T. (2000) *Bioinformatics* **16,** 404–405
37. Garnier, J., Gibrat, J. F., and Robson, B. (1996) *Methods Enzymol.* **266,** 540–553
38. Garofalo, A., Klager, S. L., Rowlinson, M. C., Nirmalan, N., Klion, A., Allen, J. E., Kennedy, M. W., and Bradley, J. E. (2002) *Mol. Biochem. Parasitol.* **122,** 161–170
39. McDermott, L., Kennedy, M. W., McManus, D. P., Bradley, J. E., Cooper, A., and Storch, J. (2002) *Biochemistry* **41,** 6706–6713
40. Tweedie, S., Paxton, W. A., Ingram, L., Maizels, R. M., McReynolds, L. A., and Selkirk, M. E. (1993) *Exp. Parasitol.* **76,** 156–164
41. Jaroszewski, L., Rychlewski, L., Li, Z., Li, W., and Godzik, A. (2005) *Nucleic Acids Res.* **33,** W284–W288
42. Torda, A. E., Procter, J. B., and Huber, T. (2004) *Nucleic Acids Res.* **32,** W532–W535
43. Kelley, L. A., MacCallum, R. M., and Sternberg, M. J. (2000) *J. Mol. Biol.* **299,** 499–520
44. McGuffin, L. J., and Jones, D. T. (2003) *Bioinformatics* **19,** 874–881
45. Shi, J., Blundell, T. L., and Mizuguchi, K. (2001) *J. Mol. Biol.* **310,** 243–257
46. Murzin, A. G., Brenner, S. E., Hubbard, T. J. P., and Chothia, C. (1995) *J. Mol. Biol.* **247,** 536–540
47. Hadley, C., and Jones, D. T. (1999) *Structure Fold. Des.* **7,** 1099–1112